RSC Advances

PAPER

View Article Online
View Journal | View Issue

Open Access Article. Published on 25 February 2026. Downloaded on 3/8/2026 1:18:58 PM.
This article is licensed under a Creative Commons Attribution-NonCommercial 3.0 Unported Licence.

Check for updates

Cite this: *RSC Adv.*, 2026, **16**, 11090

Design, synthesis, molecular docking, and antimicrobial evaluation of hybrid peptides incorporating unnatural amino acids with enhanced hydrophobic sidechains

Subhash Rao Marata,[a] Tushar Janardan Pawar,[b] Jose Luis Olivares-Romero,[c] Harun Patel,[d] Iqrar Ahmad,[d] Enrique Delgado-Alvarado,[e] Ghazala Muteeb,[f] Nagendra Govindappa,[a] Meghali Devi,[g] Siddhant V. Kokate*[h] and Lakshmi Basavegowda *[a]

Received 21st July 2025
Accepted 16th December 2025

DOI: 10.1039/d5ra05259a

rsc.li/rsc-advances

The emergence of multidrug-resistant (MDR) pathogens has intensified the need for novel antimicrobial agents. This study focuses on the design, synthesis, and evaluation of hybrid peptides (**6a–6e**) incorporating unnatural amino acids featuring enhanced hydrophobic side chains. These peptides, particularly **6e**, demonstrated potent antimicrobial efficacy. Molecular docking identified the robust binding affinities of peptides **6e** and **6b** towards the transglycosylase domain of *Escherichia coli* PBP1b, indicating their potential as enzyme inhibitors. Molecular dynamics (MD) simulations confirmed the stability of peptide-protein complexes over a 100 ns timespan, supporting the structural integrity of peptide **6e**. Experimental data further validated computational predictions, with peptide **6e** exhibiting minimum inhibitory concentrations (MICs) as low as 2 μg mL^{-1} against *E. coli* and 0.2 μg mL^{-1} against *Bacillus subtilis*. Additionally, **6e** demonstrated broad-spectrum antifungal efficacy, showing competitive activity against *Candida albicans* and *Aspergillus niger*. These results establish unnatural amino acid-based peptides as promising candidates in addressing MDR infections, warranting further studies for clinical application.

Introduction

The rapid emergence and proliferation of antibiotic-resistant bacteria has created a pressing need for new antimicrobial agents.[1] Traditional antibiotics are losing their effectiveness against a range of pathogenic bacteria, leading to a global health crisis that threatens to undermine many of the advances made in modern medicine.[2] This challenge has spurred the scientific community to explore novel approaches to combat bacterial infections, including the development of new classes of antimicrobial compounds.[3] Among these, peptides incorporating unnatural amino acids (AAs) have garnered significant attention due to their unique properties and potential to overcome some of the limitations associated with traditional antibiotics.[4]

Peptides play crucial roles in various biological processes. In the context of antimicrobial therapy, peptides can disrupt bacterial cell membranes, inhibit essential bacterial enzymes, or interfere with vital cellular processes.[5] The versatility of peptides, combined with their ability to be synthetically modified, makes them attractive candidates for developing new antimicrobial agents.[6] Unnatural amino acids, which are AAs that do not naturally occur in proteins, offer additional advantages in this regard. These AAs can be designed to enhance the stability, specificity, and activity of peptides, potentially leading to more effective antimicrobial agents.[7]

One of the key strategies in designing effective antimicrobial peptides (AMP's) is the incorporation of enhanced hydrophobic side chains.[8] Hydrophobic interactions play a significant role in the binding of peptides to bacterial membranes and proteins. By enhancing the hydrophobic character of the peptides, it is

[a]Department of Chemistry, School of Applied Science, REVA University, Bangalore-560064, India. E-mail: lakshmib@reva.edu.in
[b]Escuela de Ingeniería Química, Universidad Anáhuac Querétaro, Circuito Universidades I, Fracción 2 S/N, Zibatá, El Marqués 76246, Querétaro, Mexico
[c]Red de Estudios Moleculares Avanzados, Camps III. Instituto de Ecología, Carretera Antigua a Coatepec 351, Xalapa, 91073, Veracruz, Mexico
[d]Department of Pharmaceutical Chemistry, R. C. Patel Institute of Pharmaceutical Education and Research, Shirpur District Dhule-425405, Maharashtra, India
[e]Micro and Nanotechnology Research Center, Universidad Veracruzana, Blvd. Av. Ruiz Cortines No. 455 Fracc. Costa Verde, Boca Del R'ıo 94294, Mexico
[f]Department of Nursing, College of Applied Medical Science, King Faisal University, Al-Ahsa-31982, Saudi Arabia
[g]School of Energy Science and Engineering, Core 3, IIT Guwahati, Amingaon-781039, Assam, India
[h]Department of Chemistry, S.S.C. College, Junnar, Pune-410502, Maharashtra, India. E-mail: siddhantkokate@gmail.com

© 2026 The Author(s). Published by the Royal Society of Chemistry

Open Access Article. Published on 25 February 2026. Downloaded on 3/8/2026 1:18:58 PM.
This article is licensed under a Creative Commons Attribution-NonCommercial 3.0 Unported Licence.

possible to improve their ability to interact with and disrupt bacterial cell membranes, leading to increased antimicrobial activity. Furthermore, the inclusion of unnatural AAs and hydrophobic side chains can enhance the stability of the peptides, making them less susceptible to degradation by proteolytic enzymes.[9] The hydrophobic side chains were thus designed to serve a dual purpose: to facilitate membrane permeabilization and to enhance binding affinity with specific bacterial enzyme targets like PBP1b.

The design and synthesis of hybrid peptides incorporating unnatural AAs with enhanced hydrophobic side chains represent a promising approach to developing new antimicrobial agents. This strategy leverages the unique properties of unnatural AAs to enhance the therapeutic potential of peptides. For instance, peptides containing unnatural AAs have been shown to exhibit increased resistance to enzymatic degradation, improved membrane permeability, and enhanced binding affinity for bacterial targets.[9,10] These attributes make them highly promising candidates for the development of new antimicrobial therapies. Recently, US-FDA approved Rezafungin, a semi-synthetic cyclic peptide drug molecule used to treat candidemia and invasive candidiasis in adults. It is a long-acting echinocandin antifungal containing unnatural amino acid, 3-hydroxy-4methylproline, which helps to improve its stability against enzymatic degradation and pharmacokinetics.[10]

The integration of unnatural AAs into peptide design can significantly alter the physicochemical properties of the peptides, thereby influencing their biological activity. Unnatural AAs can introduce steric hindrance, alter electronic properties, and enhance hydrophobic interactions, all of which can contribute to increased binding affinity and specificity for bacterial targets. Crucially, these modifications can also enhance the peptide's resistance to proteolytic degradation, which is a key strategy for reducing the potential for an immunogenic response. The anti-drug antibodies (ADAs) can be caused by an immune response, which in turn reduces the effectiveness of the drug or can cause allergic responses. Therefore, it is crucial to design peptides in a such way that this potential threat of immunogenicity could be lowered. Peptides consisting of L-AAs can easily be recognised by the T- and B-cells of the immune system causing immunogenicity. The integration of unnatural AAs into peptide design can change the structure and chemical properties of the peptide, which disrupts its immune recognition. Moreover, the integration of unnatural AAs into peptides is known to disrupt their binding to Major Histocompatibility Complex (MHC) molecules and inhibiting T-cell activation, which in turn significantly reduces immunogenicity. Thus, the integration of unnatural AAs into peptide design allows for the rational design of peptides with optimized properties for antimicrobial activity.[9–11]

Recent advances in solid-phase peptide synthesis (SPPS) have facilitated the incorporation of unnatural AAs into peptide sequences.[12] SPPS is a robust and versatile technique that enables the efficient and precise assembly of peptide chains. The use of SPPS allows for the systematic introduction of unnatural AAs into specific positions within the peptide sequence, thereby enabling the fine-tuning of peptide properties. This method has been instrumental in the development of peptides with enhanced stability, activity, and selectivity.

In the quest to develop new antimicrobial agents, targeting key bacterial enzymes involved in essential cellular processes is a promising strategy. One such target is the transglycosylase domain of Penicillin-binding protein 1B (PBP1b) from *Escherichia coli*. PBP1b is a crucial enzyme involved in the biosynthesis of peptidoglycan, an essential component of the bacterial cell wall.[13] Inhibiting this enzyme can compromise the integrity of the bacterial cell wall, leading to cell death. Therefore, PBP1b represents an attractive target for the development of new antimicrobial agents.

Molecular docking studies and molecular dynamics (MD) simulations are essential computational tools in the drug discovery process, providing critical insights into the interaction patterns and stability of peptide–protein complexes.[14] Docking studies enable the prediction of binding affinity and interaction profiles of small molecules with target proteins, which helps in screening and optimizing peptide candidates before synthesis and experimental evaluation. By simulating interactions between peptides and bacterial targets, molecular docking can guide the design of novel antimicrobial agents.[15] Complementing this, MD simulations offer dynamic insights into the stability and behavior of peptide–protein complexes over time. This approach assesses structural stability, conformational changes, and interaction patterns, providing a comprehensive understanding of molecular interactions.[16] Together, these methods reveal crucial information about the flexibility, stability, and potential efficacy of peptide–protein interactions, thus informing the design and optimization of new antimicrobial peptides.

In this study, we aimed to design, synthesize, and evaluate the antimicrobial potential of hybrid peptides incorporating unnatural AAs with enhanced hydrophobic side chains. The design strategy involved incorporating hydrophobic side chains into the peptide backbone to improve interactions with bacterial membranes and enzymes. We focused on exploring the interactions of these peptides with the transglycosylase domain of PBP1b from *E. coli*, using molecular docking and MD simulations to gain insights into their binding affinity and stability. Peptide synthesis was conducted *via* SPPS, allowing precise incorporation of unnatural AAs into the sequences. By leveraging the unique properties of unnatural AAs and employing advanced computational techniques, this study seeks to contribute to the development of novel peptides as promising candidates in the fight against multi-drug-resistant bacterial and fungal pathogens.

Results and discussion

Synthesis of peptides

The synthesis of hybrid peptides incorporating unnatural AAs with enhanced hydrophobic side chains was conducted using standard SSPS techniques as shown in Scheme 1. The process began with the attachment of first AA, Alanine, to the 2-chlorotrityl chloride (2-CTC) resin giving Fmoc-Ala-CT resin **1**.

Open Access Article. Published on 25 February 2026. Downloaded on 3/8/2026 1:18:58 PM.
This article is licensed under a Creative Commons Attribution-NonCommercial 3.0 Unported Licence.

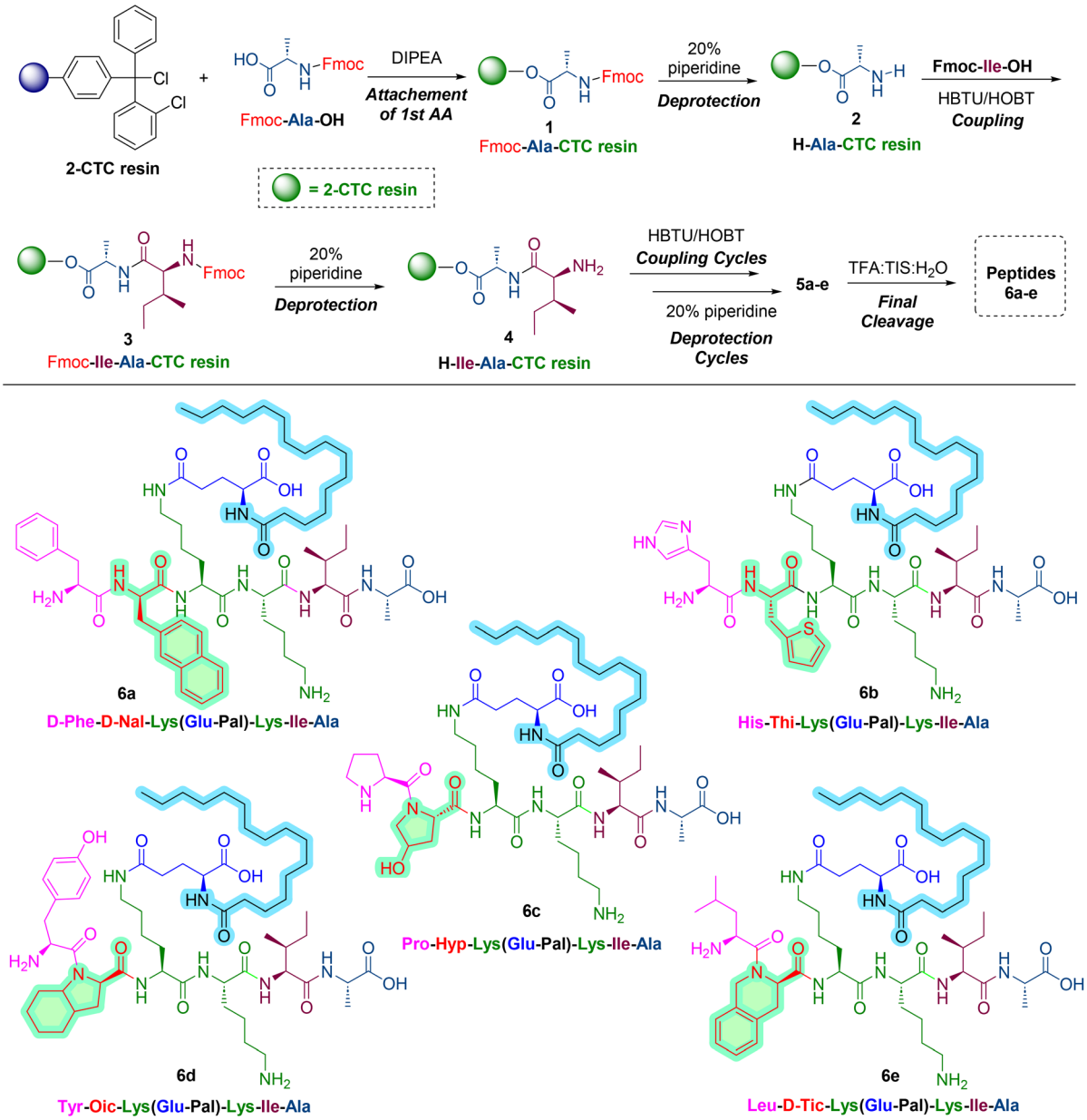

Scheme 1 Solid phase peptide synthesis of novel peptides **6a–e** derived from unnatural AAs with enhanced hydrophobic side chains.

The CTC resin is a common choice for SPPS due to its efficiency in anchoring the initial AA. The resin was thoroughly washed and swelled in dichloromethane (DCM) before the coupling of Fmoc-Ala-OH, facilitated by diisopropylethylamine (DIPEA). The successful attachment of the alanine to the resin was confirmed through UV spectrophotometry, ensuring optimal loading for subsequent peptide synthesis. The loading capacity of the resin was determined to be 0.64 mmol g^{-1}.[17]

The next phase involved the iterative coupling and deprotection cycles characteristic of SPPS. Each cycle started with the deprotection of the Fmoc group using a 20% solution of piperidine in dimethylformamide (DMF). The Fmoc protective group was removed from compound **1** yielding H-Ala-CTC resin **2**, revealing the free amino ($-NH_2$) group at its N-terminus. The successful removal of the Fmoc group was confirmed by a positive Kaiser test, indicated by the transformation of the test solution and resin to a dark blue color. After the initial deprotection, Fmoc-Ile-OH was coupled to compound **2** under conditions facilitated by HBTU/HOBt, leading to the formation of Fmoc-Ile-Ala-CTC resin **3**. The completion of this coupling reaction was verified through the Kaiser test, with a colorless test solution and resin beads indicating completion of the reaction. Further removal of the Fmoc group from compound **3** resulted in the formation of H- Fmoc-Ile-Ala-CTC resin **4**. This crucial step exposed the amino group for the subsequent coupling reaction. Each AA was coupled under these conditions, with the progress confirmed by the Kaiser test. This methodical approach allowed the sequential addition of amino acids (L/D-isomers), including unnatural ones, like, D-Nal (3-(2-Naphthyl)-D-alanine), Thi (2-Thienyl-L-alanine), Oic ((2*R*,3 a*R*,7 a*R*)-

 © 2026 The Author(s). Published by the Royal Society of Chemistry

Open Access Article. Published on 25 February 2026. Downloaded on 3/8/2026 1:18:58 PM.
This article is licensed under a Creative Commons Attribution-NonCommercial 3.0 Unported Licence.

octahydro-1*H*-indole-2-carboxylic acid), Hyp (4-*trans*-Hydroxy-L-proline), and D-Tic ((*R*)-1,2,3,4-tetrahydroisoquinoline-3-carboxylic acid), and Lys with hydrophobic side-chain designed to enhance hydrophobic interactions affording the desired peptide **5**.

The cleavage of the synthesized peptide from the resin and the removal of side-chain protecting groups (SPGs) were achieved using a cleavage cocktail of triisopropylsilane (TIS), water, and trifluoroacetic acid (TFA) in an 80 : 10 : 10 ratio, affording the desired peptide **6a**. This mixture efficiently cleaved the peptide from the resin while simultaneously removing side-chain protections. The resulting peptide was precipitated using chilled diisopropyl ether (DIPE), which facilitated their purification. The precipitated peptide was collected by filtration, washed, and dried under vacuum, yielding the final product in a powder form. Similarly, all desired peptides **6b–e** were synthesized.

The synthesized peptides were purified using preparative HPLC giving purity of 97–99% for all the peptides. All the details of the purification are provided in the supplementary information (SI) file. Moreover, the characterization of the synthesized peptides was performed to confirm their structure and purity. NMR spectroscopy, using both ^{1}H and ^{13}C NMR, provided detailed insights into the chemical structure of the peptides (Fig. S5–S14). Mass spectrometry (MS) further confirmed the molecular weights, ensuring the successful synthesis of the desired sequences (Fig. S15–S19). The purity check was carried out using analytical HPLC. HPLC spectra of all the compounds are provided in the SI file (Fig. S20–S25).

The peptide sequences synthesized in this study incorporated specific unnatural AAs to enhance their hydrophobic interactions and stability. For instance, peptides such as **6a** and **6b** were designed with hydrophobic AAs like leucine and valine to improve their interaction with bacterial membranes. Other peptides, like **6c**, **6d** and **6e**, featured strategic modifications aimed at increasing binding affinity and stability. The incorporation of these unnatural AAs was intended to create peptides with superior antimicrobial properties, capable of overcoming the limitations of traditional antibiotics.

Molecular docking

The molecular docking study was conducted to examine the binding interactions between the synthesized peptides **6a–e** and the transglycosylase domain of *E. coli* PBP1b (PDB: 3VMA), a key enzyme in peptidoglycan biosynthesis. The crystal structure of *E. coli* Penicillin-Binding Protein 1b (PBP1b) was retrieved from the Protein Data Bank (PDB ID: 3VMA) and used for molecular docking and molecular dynamics simulation studies. Inhibiting this enzyme compromises bacterial cell wall integrity, making it a valuable target for antibacterial drug development.[18]

The docking results indicate that the synthesized peptides possess significant binding affinities towards the transglycosylase domain, with peptide **6e** exhibiting the highest docking score of −6.944 kcal mol^{-1}, followed closely by **6b** with a score of −6.923 kcal mol^{-1} **6a**, **6c**, and **6d** demonstrated similar docking scores of −6.894, −6.892, and −6.889 kcal mol^{-1}, respectively, all suggesting robust interactions with the enzyme's active site. These scores are markedly more negative than that of ampicillin (−5.079 kcal mol^{-1}), indicating a lower binding affinity of the conventional antibiotic for this target. In comparison, moenomycin, a known inhibitor of the transglycosylase domain, showed the highest binding affinity with a docking score of −8.790 kcal mol^{-1}, setting a benchmark for potential inhibition efficacy (Table 1).

Table 1 Docking scores and interaction energies of synthesized peptides and ampicillin

Ligand	Docking score (kcal mol^{-1})	Glide energy (kcal mol^{-1})
Peptide **6a**	−6.894	−70.207
Peptide **6b**	−6.923	−79.278
Peptide **6c**	−6.892	−68.432
Peptide **6d**	−6.889	−66.537
Peptide 6e	**−6.944**	**−81.256**
Ampicillin	−5.079	−33.398

Detailed interaction analysis revealed that **6b** forms multiple stabilizing interactions within the transglycosylase active site, including six hydrogen bonds with residues Asn 275, Arg 325, Glu 323, Asp 321, and Arg 91, along with salt bridge interactions involving Glu 323 and Arg 94, and a π-cation interaction with Tyr 315 (Fig. S1). **6e**, which also showed a strong docking score, establishes five hydrogen bonds with residues Lys 274, Asn 275, Leu 278, and Arg 286, reinforcing its binding affinity (Fig. 1). For reference, moenomycin, the co-crystallized ligand, forms six hydrogen bonds with residues Glu 233, Gln 271, Lys 274, Asn 275, Ala 357, and Glu 323 (Fig. S2), underscoring its high affinity and inhibitory potential.

Molecular dynamics (MD) simulation

MD simulations were performed to assess the dynamic stability and behavior of the **6e** peptide within the binding site of the

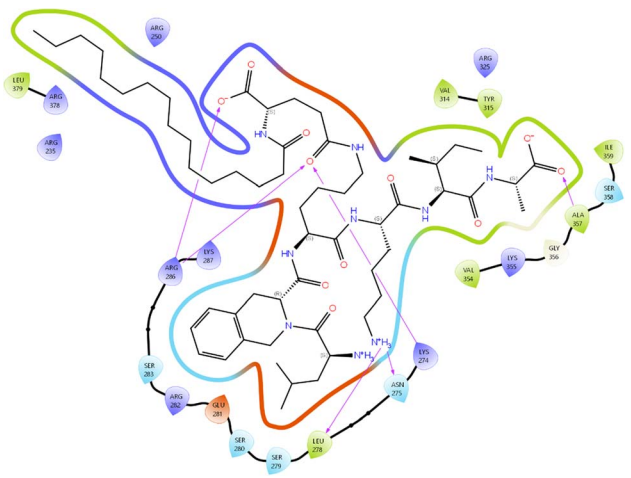

Fig. 1 Interaction of compound **6e** with transglycosylase domain of PBP1b of *E coli*.

Open Access Article. Published on 25 February 2026. Downloaded on 3/8/2026 1:18:58 PM.
This article is licensed under a Creative Commons Attribution-NonCommercial 3.0 Unported Licence.

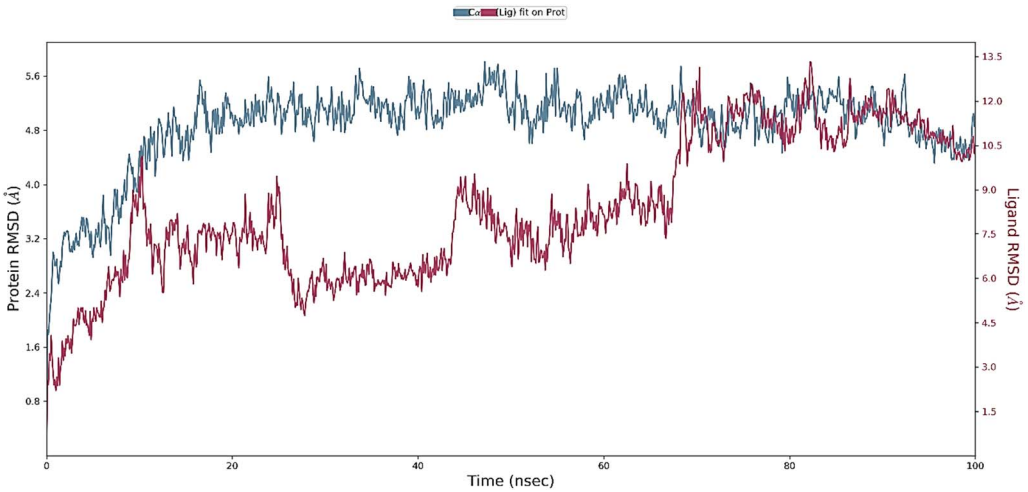

Fig. 2 Root mean square deviation (RMSD) of peptide **6e** with transglycosylase for the 100 ns molecular dynamics simulation.

transglycosylase domain of *E. coli* PBP1b over a 100 ns period. While docking provides a static snapshot of binding affinity, MD simulations allow for the evaluation of structural stability and flexibility in a dynamic environment, offering deeper insights into the peptide–protein interactions.[19]

Root-Mean-Square Deviation (RMSD) was analyzed as a primary metric of complex stability.[20] For the protein, RMSD values initially rose from 1.8 Å to a peak of 5.54 Å within the first 18 ns, after which stabilization occurred between 4.61 Å and 5.81 Å until 68 ns. A notable fluctuation at 68.3 ns reached 5.74 Å, followed by a stable range between 4.68 Å and 5.63 Å for the remainder of the simulation. The ligand's RMSD, observed on the right *Y*-axis, revealed substantial fluctuations. From 0 to 10 ns, the RMSD increased to 8.34 Å, with further peaks and troughs, reaching a significant peak of 13.13 Å at 70 ns. In the final phase of the simulation (87–100 ns), the ligand RMSD stabilized between 10.5 Å and 13.5 Å, ultimately settling at 10.5 Å (Fig. 2).

Root-Mean-Square Fluctuation (RMSF) analysis was performed to evaluate the flexibility of specific protein residues during the simulation.[21] High RMSF values corresponded to flexible regions, while low RMSF values indicated rigid segments. Throughout the simulation, the **6e** peptide interacted with 52 AAs within the binding site, with notable interactions involving residues such as Arg94 (2.07 Å), Leu278 (2.75 Å), Ser279 (2.84 Å), Ser280 (3.41 Å), and Arg286 (3.07 Å), among others (Fig. 3). Regions with elevated RMSF values highlighted areas of increased flexibility, which may contribute to binding stability and adaptability within the active site.

A detailed analysis of **6e** protein–ligand interactions throughout the simulation revealed four primary categories of contacts: hydrogen bonds, hydrophobic interactions, ionic interactions, and water-mediated hydrogen bonds. This categorization provided insights into the stability and persistence of interactions that contribute to the binding efficacy of **6e**. For quantitative assessment, interaction frequencies were visualized using normalized stacked bar charts over the simulation trajectory, where a value of 0.6 indicated that a specific interaction was present for 60% of the simulation time. This visualization highlighted the temporal stability of key interactions, shedding light on the dynamics of protein-ligand binding.

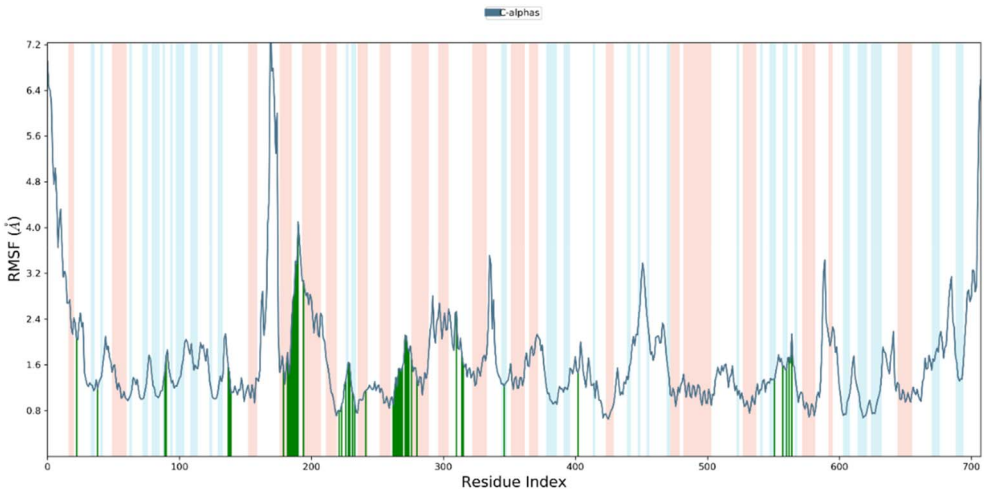

Fig. 3 Root mean square fluctuation (RMSF) of transglycosylase in complex with peptide **6e**.

 © 2026 The Author(s). Published by the Royal Society of Chemistry

Open Access Article. Published on 25 February 2026. Downloaded on 3/8/2026 1:18:58 PM.
This article is licensed under a Creative Commons Attribution-NonCommercial 3.0 Unported Licence.

The **6e** peptide demonstrated consistent hydrogen bonding with critical residues such as Glu281, Arg282, Glu323, and Arg364, underscoring their roles in stabilizing the complex. Significant hydrophobic interactions, particularly with residue Tyr315, contributed to **6e**'s binding affinity. Ionic interactions involving residues Arg281 and Glu323 further reinforced the stability of the complex. Additionally, water-mediated hydrogen bonds with residues Glu211, Asn275, Arg281, Gln318, Glu323, and Ser358 illustrated the intricate network of interactions essential to the functionality of the **6e**–protein complex.

The MD simulation results provide detailed information about dynamic stability and flexibility of the **6e** peptide within the binding site, reinforcing the initial docking results and supporting its potential as a stable inhibitor of the transglycosylase domain in *E. coli*.

MD simulation of compound **6e** was further compared with the ampicillin–transglycosylase PBP1b (3VMA) complex. The RMSD analysis of the ampicillin–transglycosylase PBP1b (3VMA) complex was conducted to assess the dynamic stability and conformational behavior over a 100 ns molecular dynamics simulation. The Cα RMSD of the protein exhibited an initial rise during the first 10 ns, followed by mild fluctuations and eventual stabilization around 4.7–5.2 Å after 40 ns, indicating that the protein retained its overall structural integrity throughout the simulation. The ligand RMSD displayed an early increase within the first 20 ns, suggesting the adjustment of ampicillin within the binding pocket, and subsequently major fluctuation observed between 2.5–4.8 Å from 30 ns to 75 ns, and from 76 ns onward ampicillin RMSD stabilized in the transglycosylase enzyme (Fig. 4).

The Root Mean Square Fluctuation analysis of the transglycosylase PBP1b (3VMA) protein complexed with ampicillin over a 100 ns molecular dynamics simulation provided detailed insights into the residue-wise flexibility and stability of the complex. The RMSF values for the active site domain fell within a moderate range, with distinct peaks around residue indices 100, 200, 300, and 400, highlighting flexible regions that contribute to the protein's dynamic behavior. Ampicillin interacted with 39 key residues of the Trans glycosylase PBP1b protein, including Tyr83 (3.74 Å), Val85 (3.06 Å), Tyr86 (3.18 Å), Asp234 (3.23 Å), Arg234 (5.17 Å), Arg256 (1.92 Å), Gln270 (1.63 Å), Lys274 (1.53 Å), Leu278 (2.65 Å), Ser279 (5.13 Å), Ser280 (5.13 Å), Glu281 (5.07 Å), Arg282 (4.40 Å), Ser283 (3.89 Å), Tyr284 (4.43 Å), Trp285 (3.98 Å), Arg286 (2.89 Å), Lys287 (3.44 Å), Leu309 (1.77 Å), Glu313 (1.21 Å), Glu323 (1.57 Å), Met353 (1.39 Å), Val354 (1.33 Å), Lys355 (1.58 Å), Gly356 (1.73 Å), Trp532 (1.58 Å), Ile533 (1.58 Å), Ala534 (1.76 Å), Asp535 (1.17 Å), Ala536 (1.94 Å), Pro537 (2.06 Å), Arg555 (1.95 Å), Glu559 (2.32 Å), Gly561 (2.10 Å), Arg569 (1.03 Å), Val578 (1.32 Å), Gly767 (2.08 Å), Tyr770 (2.24 Å), and Gly779 (2.25 Å) (Fig. 5).

The protein–ligand contact analysis of the transglycosylase PBP1b protein complexed with ampicillin revealed hydrogen bonds and water-mediated interactions played a dominant role, with residues Lys247, Ser270, Arg286 (35%), and Arg502. Overall comparison showed that compound **6e** is more stable as compared to the ampicillin.

Biological evaluation

The synthesized peptides exhibited significant antimicrobial activity against a broad spectrum of bacterial and fungal pathogens. Initial molecular docking studies suggested strong binding affinities of these peptides to the transglycosylase domain of *E. coli PBP1b*, a key bacterial enzyme. Notably, **6e** demonstrated the highest binding affinity with a docking score of −6.944 kcal mol^{-1}, outperforming the reference antibiotic ampicillin (−5.079 kcal mol^{-1}). This high affinity is attributed

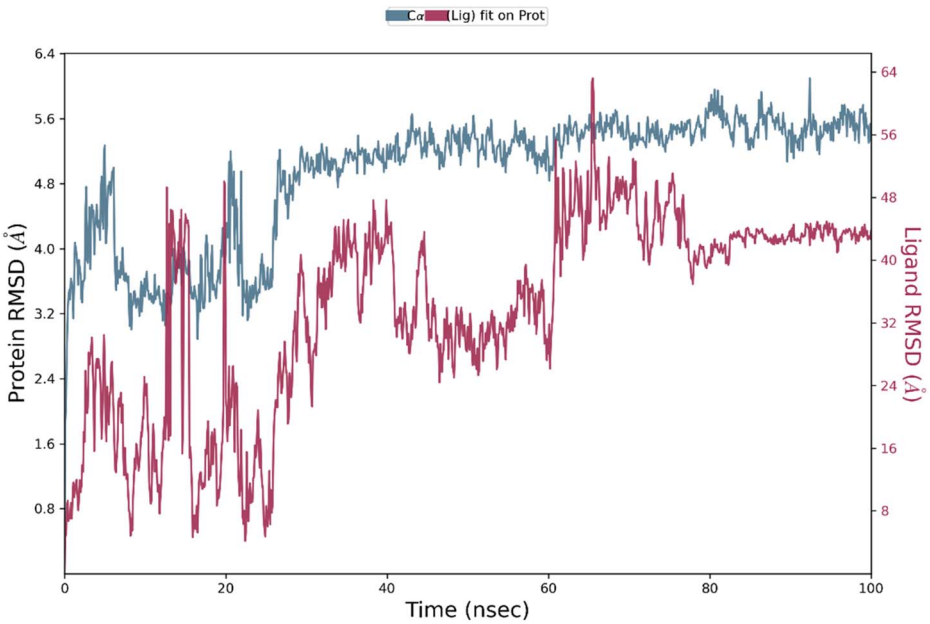

Fig. 4 Root mean square deviation (RMSD) of ampicillin with transglycosylase for the 100 ns molecular dynamics simulation.

Open Access Article. Published on 25 February 2026. Downloaded on 3/8/2026 1:18:58 PM.
This article is licensed under a Creative Commons Attribution-NonCommercial 3.0 Unported Licence.

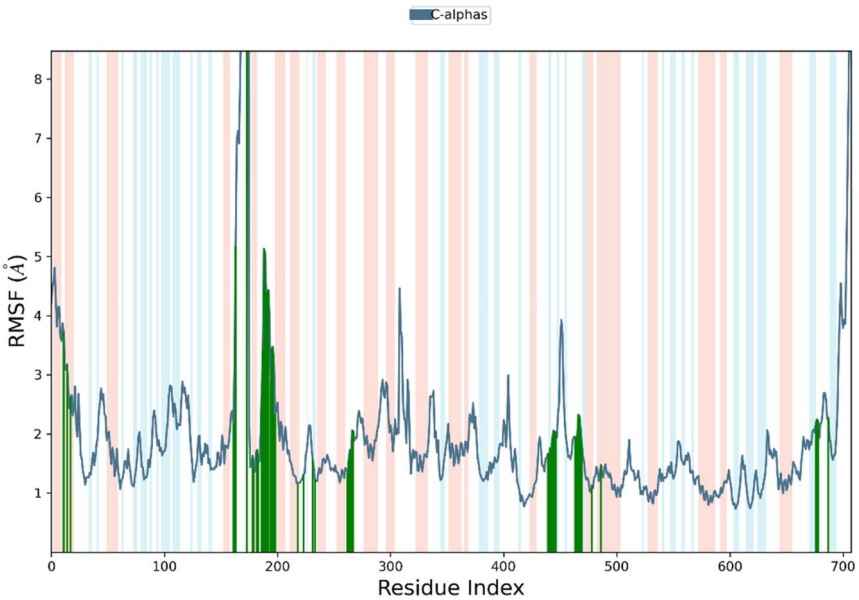

Fig. 5 Root mean square fluctuation (RMSF) of transglycosylase in complex with ampicillin.

to multiple hydrogen bonds formed with active site residues Lys274, Asn275, Leu278, and Arg286, highlighting its potential to inhibit enzyme activity effectively.

Biological assays validated these computational insights, showing that **6e** had potent antibacterial effects with a minimum inhibitory concentration (MIC) of 2 μg mL^{-1} against *E. coli*, a twofold improvement over ampicillin (MIC of 4 μg mL; Table 2 and Fig. 6). Additionally, **6e** demonstrated excellent activity against *Bacillus subtilis* with an MIC of 0.2 μg mL^{-1}, surpassing ampicillin, which had an MIC of 0.5 μg mL^{-1}. The peptide also exhibited strong activity against *Bacillus megaterium* and *Streptococcus pyogenes*, with MIC values of 0.3 μg mL^{-1} each, which are favorable compared to ampicillin's MICs of 0.5 μg mL^{-1} and 0.2 μg mL^{-1}, respectively.

Other synthesized peptides, such as **6b** and **6c**, also displayed notable antibacterial activities. For example, peptide **6b** exhibited an MIC of 3 μg mL^{-1} against *E. coli* and 0.3 μg mL^{-1} against *B. subtilis*, while peptide **6c** showed MIC values of 4 μg mL^{-1} and 0.3 μg mL^{-1} against *E. coli* and *B. subtilis*, respectively. Both peptides demonstrated comparable activity against *B. megaterium* and *S. pyogenes*, with MIC values ranging from 0.5 to 0.8 μg mL^{-1}, underscoring their efficacy against a range of Gram-positive and Gram-negative bacteria.

In addition to antibacterial activity, the peptides were tested for antifungal efficacy. Peptide **6e** emerged as the most potent antifungal agent, with MIC values of 7.5 μg mL^{-1} against *Aspergillus niger*, 8 μg mL^{-1} against *Aspergillus oryzae*, and 8 μg mL^{-1} against *Rhizopus* spp., performing on par with or better than the standard antifungal agent fluconazole, which exhibited MIC values of 8, 9.5, and 9.5 μg mL^{-1}, respectively. Furthermore, peptide **6e** showed strong activity against *Candida albicans* with an MIC of 2 μg mL^{-1}, matching the efficacy of fluconazole.

Notably, demonstrated the highest binding affinity with a docking score of −6.944 kcal mol^{-1}, outperforming the reference antibiotic ampicillin (−5.079 kcal mol^{-1}). This highest affinity is attributed to a robust and stable interaction network established within the transglycosylase active site. Specifically, forms five critical hydrogen bonds with residues Lys274, Asn275, Leu278, and Arg286, a network reinforced by

Table 2 MIC values (in μg mL^{-1}) for five peptides **6a–e** and two standard compounds (ampicillin for antibacterial and fluconazole for antifungal testing)

Compounds	*E. coli*[a]	*B. subtilis*[a]	*B. megaterium*[a]	*S. pyogenes*[a]	*A. niger*[b]	*A. oryzae*[b]	*Rhizopus* spp.[b]	*C. albicans*[b]
6a	5	0.4	0.7	0.7	9	9	10	3
6b	3	0.3	0.5	0.6	8	8.5	9.5	2.5
6c	4	0.3	0.6	0.6	8.5	8.5	10	3
6d	6	0.5	1	0.6	10	10.5	11	3.5
6e	2	0.2	0.3	0.3	7.5	8	8	2
Ampicillin	4	0.5	1	0.2	—	—	—	—
Fluconazole	—	—	—	—	8	9.5	9.5	2

[a] Antibacterial activity. [b] Antifungal activity.

 © 2026 The Author(s). Published by the Royal Society of Chemistry

Open Access Article. Published on 25 February 2026. Downloaded on 3/8/2026 1:18:58 PM.
This article is licensed under a Creative Commons Attribution-NonCommercial 3.0 Unported Licence.

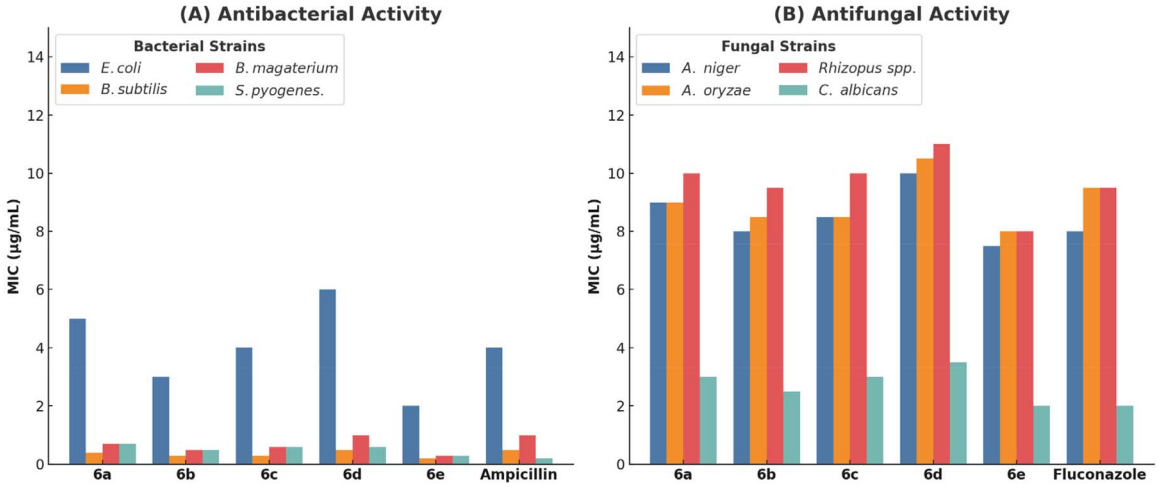

Fig. 6 *In vitro* antimicrobial activity measured by MIC (μg mL^{-1}) of peptides **6a–e** against bacterial and fungal strains. (A) Antibacterial activity against bacterial strains (*E. coli, B. subtilis, B. megaterium, S. pyogenes*), ampicillin as a standard. (B) Antifungal activity against fungal strains (*A. niger, A. oryzae, Rhizopus* spp., *C. albicans*), fluconazole as a standard.

significant hydrophobic interactions with Tyr315 and ionic interactions involving Glu281 and Arg364, as confirmed by molecular dynamics simulations. This specific and stable binding pattern, particularly involving key residues that facilitate enzyme inhibition, is the structural foundation for **6e**'s superior potency. Biological assays validated these computational insights, showing that **6e** had potent antibacterial effects with a MIC of 2 μg mL^{-1} against *E. coli*, a twofold improvement over ampicillin (4 μg mL^{-1}).

While the potent antibacterial activity is linked to the inhibition of the *E. coli* PBP1b enzyme, the observed broad-spectrum antifungal activity, particularly against strains like *A. niger* and *C. albicans* suggests a different mode of action. Fungal pathogens lack the PBP1b enzyme; therefore, the computational studies targeting this protein are not directly applicable to their mechanism of inhibition. The antifungal efficacy is likely attributed to a membrane-disrupting mechanism, which is a common characteristic of antimicrobial peptides (AMPs). The strategic incorporation of enhanced hydrophobic side chains (such as in the Lys (Glu−Pal) residue) in our hybrid peptides is designed to facilitate strong hydrophobic interactions with the fungal cell membrane lipids, leading to destabilization and subsequent cell death. This dual mechanism (enzyme inhibition for bacteria and membrane disruption for fungi) underscores the versatility and promising broad-spectrum profile of the synthesized peptides.

Other peptides demonstrated moderate to good antifungal activity. For instance, peptide **6b** showed MIC values of 8 μg mL^{-1} against *A. niger*, 8.5 μg mL^{-1} against *A. oryzae*, and 9.5 μg mL^{-1} against *Rhizopus* spp., while maintaining an MIC of 2.5 μg mL^{-1} against *C. albicans*. Peptide **6a** displayed similar antifungal activity, with MIC values of 9 μg mL^{-1} against *A. niger* and *A. oryzae*, and 10 μg mL^{-1} against *Rhizopus* spp., alongside an MIC of 3 μg mL^{-1} against *C. albicans*. These results indicate that the synthesized peptides, especially **6e**, exhibit broad-spectrum antimicrobial properties with potent activities against both bacterial and fungal pathogens, positioning them as promising candidates for further development as antimicrobial agents (Table 2).

The integration of molecular docking, MD simulations, and biological activity assessments provided a comprehensive evaluation of the synthesized peptides' potential as antimicrobial agents. The molecular docking studies identified strong binding affinities, particularly for peptides **6e** and **6b**, towards the transglycosylase domain of *E. coli* PBP1b, suggesting their promise as effective enzyme inhibitors. These predictions were further substantiated by MD simulations, which demonstrated the stability and adaptability of these peptide–enzyme interactions over time, reinforcing their potential inhibitory capacity. Biological assays aligned closely with the computational predictions, revealing potent antimicrobial activity of the peptides against a spectrum of bacterial and fungal pathogens, often surpassing conventional antibiotics in effectiveness. These congruent results underscore the reliability of combining computational and experimental approaches in guiding the rational design of novel antimicrobial agents.

Conclusions

This research presents compelling evidence of the antimicrobial potential of peptides synthesized from unnatural amino acids with hydrophobic enhancements. Both computational and biological assessments underline the efficacy of these peptides, especially compound **6e**, as potent agents against a range of bacterial and fungal pathogens. Molecular docking and MD simulations reveal strong binding and structural stability, highlighting their mechanism of action and durability as inhibitors. The pronounced antibacterial and antifungal activities, observed *in vitro*, support the strategic integration of unnatural amino acids to improve peptide functionality. Given these promising results, these peptides offer a viable pathway toward developing new therapeutics targeting MDR pathogens.

Open Access Article. Published on 25 February 2026. Downloaded on 3/8/2026 1:18:58 PM. This article is licensed under a Creative Commons Attribution-NonCommercial 3.0 Unported Licence.

Further optimization and clinical trials will be essential to translate these findings into practical applications.

Author contributions

S. R. M.: conceptualization, methodology, writing-original draft. T. J. P.: formal analysis, biological evaluation. J. L. O.-R.: formal analysis. I. A.: computing resources. H. P.: computing resources. E. D.-A.: biological evaluation. G. M.: funding acquisition. N. G.: visualization. M. D.: data curation, computing resources. S. V. K.: project administration, conceptualization, methodology, writing-original draft, review, editing. L. B.: conceptualization, methodology, writing-original draft, review, editing. All authors have read and agreed to the submitted version of the manuscript.

Conflicts of interest

There are no conflicts to declare.

Data availability

The authors confirm that the data supporting the findings of this study are available within the article and its supplementary information (SI) file, which is provided separately. No additional source data are required. Supplementary information is available. See DOI: https://doi.org/10.1039/d5ra05259a.

Acknowledgements

This work was supported by the Deanship of Scientific Research, Vice Presidency for Graduate Studies and Scientific Research, King Faisal University, Saudi Arabia [Grant No. KFU254414].

References

1 (*a*) Y. Wang and T. Dagan, *Nat. Commun.*, 2024, **15**, 4555; (*b*) X. Li, H. Hu, Y. Zhu, T. Wang, Y. Lu, X. Wang, Z. Peng, M. Sun, H. Chen, J. Zheng and C. Tan, *Nat. Commun.*, 2024, **15**, 5811; (*c*) L. Guan, M. Beig, L. Wang, T. Navidifar, S. Moradi, F. M. Tabaei, Z. Teymouri, M. A. Moghadam and M. Sedighi, *Ann. Clin. Microbiol. Antimicrob.*, 2024, **23**, 80; (*d*) J. M. Pérez de la Lastra, S. J. T. Wardell, T. Pal, C. de la Fuente-Nunez and D. Pletzer, *J. Med. Syst.*, 2024, **48**, 71; (*e*) K. Zhao, C. Li and F. Li, *Sci. Rep.*, 2024, **14**, 9719.

2 (*a*) A.-P. Magiorakos, A. Srinivasan, R. B. Carey, Y. Carmeli, M. E. Falagas, C. G. Giske, S. Harbarth, J. F. Hindler, G. Kahlmeter, B. Olsson-Liljequist, D. L. Paterson, L. B. Rice, J. Stelling, M. J. Struelens, A. Vatopoulos, J. T. Weber and D. L. Monnet, *Clin. Microbiol. Infect.*, 2012, **18**, 268; (*b*) M. Tilahun, B. Sharew and A. Shibabaw, *BMC Microbiol.*, 2024, **24**, 339; (*c*) M. Sitohy, G. Enan, S. Abdel-Shafi, N. A. El-Wafa, N. El-Gazzar, A. Osman and B. Sitohy, *BMC Microbiol.*, 2024, **24**, 49; (*d*) B. Neil, G. L. Cheney, J. A. Rosenzweig, J. Sha and A. K. Chopra, *Appl. Microbiol. Biotechnol.*, 2024, **108**, 205.

3 (*a*) T. M. Belete, *Hum. Microbiome J.*, 2019, **11**, 100052; (*b*) M. Miethke, M. Pieroni, T. Weber, M. Brönstrup, P. Hammann, L. Halby, P. B. Arimondo, P. Glaser, B. Aigle, H. B. Bode, R. Moreira, Y. Li, A. Luzhetskyy, M. H. Medema, J.-L. Pernodet, M. Stadler, J. R. Tormo, O. Genilloud, A. W. Truman, K. J. Weissman, E. Takano, S. Sabatini, E. Stegmann, H. Brötz-Oesterhelt, W. Wohlleben, M. Seemann, M. Empting, A. K. H. Hirsch, B. Loretz, C.-M. Lehr, A. Titz, J. Herrmann, T. Jaeger, S. Alt, T. Hesterkamp, M. Winterhalter, A. Schiefer, K. Pfarr, A. Hoerauf, H. Graz, M. Graz, M. Lindvall, S. Ramurthy, A. Karlén, M. van Dongen, H. Petkovic, A. Keller, F. Peyrane, Z. Donadio, L. Fraisse, L. J. V. Piddock, I. H. Gilbert, H. E. Moser and R. Müller, *Nat. Rev. Chem.*, 2021, **5**, 726.

4 (*a*) R. Oliva, M. Chino, K. Pane, V. Pistorio, A. De Santis, E. Pizzo, G. D'Errico, V. Pavone, A. Lombardi, P. Del Vecchio, E. Notomista, F. Nastri and L. Petraccone, *Sci. Rep.*, 2018, **8**, 8888; (*b*) J. Lu, H. Xu, J. Xia, J. Ma, J. Xu, Y. Li and J. Feng, *Front. Microbiol.*, 2020, **11**, 563030; (*c*) X. Wang, X. Yang, Q. Wang and D. Meng, *Crit. Rev. Microbiol.*, 2022, **49**, 231.

5 (*a*) T. Li, X. Ren, X. Luo, Z. Wang, Z. Li, X. Luo, J. Shen, Y. Li, D. Yuan, R. Nussinov, X. Zeng, J. Shi and F. Cheng, *Nat. Commun.*, 2024, **15**, 7538; (*b*) S. He and C. M. Deber, *Sci. Rep.*, 2024, **14**, 1894; (*c*) S. R. Tivari, S. V. Kokate, M. S. Gayke, I. Ahmad, H. Patel, S. G. Kumar and Y. Jadeja, *ChemistrySelect*, 2022, **7**, e202203462; (*d*) U. L. Urmi, A. K. Vijay, R. Kuppusamy, S. Islam and M. D. P. Willcox, *Peptides*, 2023, **166**, 171024; (*e*) A. Vedadghavami, C. Zhang and A. G. Bajpayee, *Nanotoday*, 2020, **34**, 100898.

6 (*a*) Z. Cheng, B.-B. He, K. Lei, Y. Gao, Y. Shi, Z. Zhong, H. Liu, R. Liu, H. Zhang, S. Wu, W. Zhang, X. Tang and Y.-X. Li, *Nat. Commun.*, 2024, **15**, 4901; (*b*) K. N. Bhaumik, R. Spohn, A. Dunai, L. Daruka, G. Olajos, F. Zákány, A. Hetényi, C. Pál and T. A. Martinek, *Commun. Biol.*, 2024, **7**, 1264; (*c*) S. R. Tivari, S. V. Kokate, E. M. Sobhia, S. G. Kumar, U. B. Shelar and Y. Jadeja, *ChemistrySelect*, 2022, **7**, e202201481; (*d*) S. R. Tivari, S. V. Kokate, U. B. Shelar and Y. Jadeja, *Rasayan J. Chem.*, 2022, **15**, 875.

7 (*a*) M. Pigula, Y.-C. Lai, M. Koh, C. S. Diercks, T. F. Rogers, D. A. Dik and P. G. Schultz, *Nat. Commun.*, 2024, **15**, 6766; (*b*) J. Lu, H. Xu, J. Xia, J. Ma, J. Xu, Y. Li and J. Feng, *Front. Microbiol.*, 2020, **11**, 563030; (*c*) S. Mitra, M.-T. Chen, F. Stedman, J. Hernandez, G. Kumble, X. Kang, C. Zhang, G. Tang, I. Daugherty, W. Liu, J. Ocloo, K. R. Klucznik, A. A. Li, F. Heinrich, B. Deslouches and S. Tristram-Nagle, *J. Phys. Chem. B*, 2024, **128**, 9772.

8 (*a*) W. Li, F. Separovic, N. M. O'Brien-Simpson and J. D. Wade, *Chem. Soc. Rev.*, 2021, **50**, 4932; (*b*) C. Zhong, N. Zhu, Y. Zhu, T. Liu, S. Gou, J. Xie, J. Yao and J. Ni, *Eur. J. Pharm. Sci.*, 2020, **141**, 105123; (*c*) J. Lu, H. Xu, J. Xia, J. Ma, J. Xu, Y. Li and J. Feng, *Front. Microbiol.*, 2020, **11**, 563030; (*d*) M. Wenzel, P. Schriek, P. Prochnow, H. B. Albada, N. Metzler-Nolte and J. E. Bandow, *Biochim. Biophys. Acta Biomembr.*, 2016, **1858**, 1004; (*e*) E. N. Lorenzón, N. A. Santos-Filho, M. A. S. Ramos,

 © 2026 The Author(s). Published by the Royal Society of Chemistry

Open Access Article. Published on 25 February 2026. Downloaded on 3/8/2026 1:18:58 PM.
This article is licensed under a Creative Commons Attribution-NonCommercial 3.0 Unported Licence.

T. M. Bauab, I. L. B. C. Camargo and E. M. Cilli, *Protein Pept. Lett.*, 2016, **23**, 738.

9 (*a*) O. Al Musaimi, L. Lombardi, D. R. Williams and F. Albericio, *Pharmaceuticals*, 2022, **15**, 1283; (*b*) F. Taherali, N. Chouhan, F. Wang, S. Lavielle, M. Baran, L. E. McCoubrey, A. W. Basit and V. Yadav, *Pharmaceutics*, 2023, **15**, 1956; (*c*) P. Gagat, M. Ostrówka, A. Duda-Madej and P. Mackiewicz, *Int. J. Mol. Sci.*, 2024, **25**, 10821.

10 (*a*) R. Oliva, M. Chino, K. Pane, V. Pistorio, A. De Santis, E. Pizzo, G. D'Errico, V. Pavone, A. Lombardi and P. Del Vecchio, *Sci. Rep.*, 2018, **8**, 8888; (*b*) A. R. D'Souza, M. R. Necelis, A. Kulesha, G. A. Caputo and O. V. Makhlynets, *Biomolecules*, 2021, **11**, 421; (*c*) O. Al Musaimi, *Antibiotics*, 2025, **14**, 166; (*d*) Y. Y. Syed, *Drugs*, 2023, **83**, 833.

11 (*a*) X. Wang, X. Yang, Q. Wang and D. Meng, *Crit. Rev. Microbiol.*, 2023, **49**, 231; (*b*) G. N. Enninful, R. Kuppusamy, E. K. Tiburu, N. Kumar and M. D. P. Willcox, *J. Pept. Sci.*, 2024, **30**, e3560; (*c*) A. E. Mattei, A. H. Gutierrez, W. D. Martin, F. E. Terry, B. J. Roberts, A. S. Rosenberg and A. S. de Groot, *Front. Drug Discov.*, 2022, **2**, 952326; (*d*) A. Azam, S. Mallart, S. Illiano, O. Duclos, C. Prades and B. Mallere, *Front. Immunol.*, 2021, **12**, 637963.

12 (*a*) G. Rossino, E. Marchese, G. Galli, F. Verde, M. Finizio, M. Serra, P. Linciano and S. Collina, *Molecules*, 2023, **28**, 7165; (*b*) A. R. Paquette and C. N. Boddy, *Org. Biomol. Chem.*, 2023, **21**, 8043; (*c*) J. Zou, M. Zhou, X. Xiao and R. Liu, *Macromol. Rapid Commun.*, 2022, **23**, 2200575.

13 (*a*) A. J. F. Egan, B. Jacob, I. van't Veer, E. Breukink and W. Vollmer, *Phil. Trans. R. Soc. B*, 2015, **370**, 20150031; (*b*) A. Galinier, C. Delan-Forino, E. Foulquier, H. Lakhal and F. Pompeo, *Biomolecules*, 2023, **13**, 720; (*c*) A. J. F. Egan, R. Maya-Martinez, I. Ayala, C. M. Bougault, M. Banzhaf, E. Breukink, W. Vollmer and J.-P. Simorre, *Mol. Microb.*, 2018, **110**, 335.

14 (*a*) H. M. Patel, M. Palkar and R. Karpoormath, *Chem. Biodivers.*, 2020, **17**, e2000237; (*b*) J. A. Agwupuye, H. Louis, T. E. Gber, I. Ahmad, E. C. Agwamba, A. B. Samuel, E. J. Ejiako, H. Patel, I. T. Ita and V. M. Bassey, *Chem. Phys. Impact*, 2022, **5**, 100122; (*c*) R. Pawara, I. Ahmad, D. Nayak, S. Wagh, A. Wadkar, A. Ansari, S. Belamkar, S. Surana, C. Nath Kundu, C. Patil and H. Patel, *Bioorg. Chem.*, 2021, **115**, 105234.

15 (*a*) S. R. Tivari, S. V. Kokate, E. Delgado-Alvarado, M. S. Gayke, A. Kotmale, H. Patel, I. Ahmad, E. M. Sobhia, S. G. Kumar, B. G. Lara, V. D. Jain and Y. Jadeja, *RSC Adv.*, 2023, **13**, 24250; (*b*) Y. O. Ayipo, I. Ahmad, Y. S. Najib, S. K. Sheu, H. Patel and M. N. Mordi, *J. Biomol.Struct. Dyn.*, 2022, **5**, 1959.

16 (*a*) S. R. Tivari, S. V. Kokate, J. L. Belmonte-Vázquez, T. J. Pawar, H. Patel, I. Ahmad, M. S. Gayke, R. S. Bhosale, V. D. Jain, G. Muteeb, E. Delgado-Alvarado and Y. Jadeja, *ACS Omega*, 2023, **8**, 48843; (*b*) I. Ahmad, H. Jadhav, Y. Shinde, V. Jagtap, R. Girase and H. Patel, *In Silico Pharmacol*, 2021, **9**, 1.

17 P. K. Chandole, T. J. Pawar, J. L. Olivares-Romero, S. R. Tivari, B. G. Lara, H. Patel, I. Ahmad, E. Delgado-Alvarado, S. V. Kokate and Y. Jadeja, *RSC Adv.*, 2024, **14**, 17710.

18 (*a*) D. T. King, G. A. Wasney, M. Nosella, A. Fong and N. C. J. Strynadk, *J. Biol. Chem.*, 2017, **3**, 979; (*b*) F. Sun, Y. Sun, Y. Wang, Q. Yuan, L. Xiong, W. Feng and P. Xia, *Curr. Microbiol.*, 2022, **79**, 271.

19 I. Ahmad, D. Kumar and H. Patel, *J. Biomol. Struct. Dyn.*, 2022, **40**, 7991.

20 (*a*) Y. O. Ayipo, I. Ahmad, W. Alananzeh, A. Lawal, H. Patel and M. N. Mordi, *J. Biomol. Struct. Dyn.*, 2022, **29**, 1; (*b*) N. C. Desai, A. S. Maheta, A. M. Jethawa, U. P. Pandit, I. Ahmad and H. Patel, *J. Heterocycl. Chem.*, 2022, **59**, 879.

21 (*a*) C. T. Walsh, *Nat. Prod. Rep.*, 2023, **40**, 326; (*b*) C. Chen, J. Hu, S. Zhang, P. Zhou, X. Zhao, H. Xu, X. Zhao, M. Yaseen and J. R. Lu, *Biomaterials*, 2012, **33**, 592.

© 2026 The Author(s). Published by the Royal Society of Chemistry